H-006

Automatic Water Body Detection in High-resolution Stereo Aerial Images

Jing Wang† Hirokazu Koizumi† Toshiyuki Kamiya†

Abstract

Water body detection in high-resolution aerial images is quite different from that in low-resolution aerial images because of the color, shape and size varieties of water bodies. In this paper, an automatic water body detection method based on stereo processing and analysis of aerial images is proposed. Firstly, a score based on the special color and disparity distribution pattern of water bodies is proposed to acquire the potential water regions. Then the matching correlation values of the pixels in the potential water regions are studied to finally extract the real water bodies. Experimental results show the effectiveness of the proposed method in detecting water bodies of various color, shape and size efficiently.

1. Introduction

Aerial image understanding has been an important topic recently for its wide application in GIS related fields such as building and updating maps, city planning, environmental management, and so on. The focus of this paper is automatic detection of water body, one of the most essential terrain features, from high-resolution aerial images.

To detect water body in aerial image is significant not only in digital mapping, but also in water pollution analysis, flood control, water conservancy management, etc. [1, 2] Besides, the comparison between the water bodies respectively detected from images of different years shows the change of river ways or lake areas, and thus helps to perform environmental analysis [3].

To automatically detect water bodies in the high-resolution aerial image with high precision is a challenging problem. Firstly, water bodies are quite diverse in color, shape and size, with many different patterns like river, lake, pond, sea and pool. Secondly, in images with resolution like 20cm, the existing detailed shape and texture features make it more difficult to carry out the precise detection.

Current methods of water body detection mainly perform in single aerial image. According to our investigation, this paper is the first one to address the topic of water body detection with stereo images by using the stereo matching features like disparity and correlation value. Experimental results show the effectiveness of the proposed in detecting various water bodies in an efficient way.

2. Related Works

The early researches of water body detection on low-resolution remote sensing images modeled the rivers as linear objects. In 1970s, VanderBrug [4], Bajcsy and Tavakoli [5] conducted such researches on Lanndsat-1 images. The linear object model has also been recently extended to extract river networks by Sollie and Grazzini [6].

Advances in sensor technology for earth observation make it possible to collect multi-spectral remote sensing images with much higher resolution like IKONOS, QuickBird, etc. With such satellite images, water bodies are usually extracted as one kind of terrestrial features in land cover classification and terrestrial object recognition [7]. Different features like color, texture, shape, edge and shadow may be utilized for the pixel classification or region segmentation. At the same time, there are both unsupervised classification methods such as maximum likelihood [7, 8] and supervised methods like SVM [9] used for water body area extraction. On the other hand, Zhang et al. studied water bodies specifically on the region contours by fast matching level set method [10]. Nath et al. provided a good review on the water body extraction methods from high-resolution satellite image [9].

To fully make use of the respective advantage, there are also several methods integrating high and low resolution images to extract water bodies [8, 11]. Dillabaugh et al. proposed a 2-stage multi-resolution strategy to firstly acquire river contours on the low resolution 20m SPOT image and then refined the contours by Snakes model on panchromatic KFA1000 images with 5m resolution [11]. Geneletti et al. made use of the multi-spectral information in the low resolution Landsat TM image to perform land cover classification and then mapped the result on the high-resolution single banded image like aerial orthophoto or SPOT panchromatic data [8]. One drawback of these methods is the requirement of image registration.

The purpose of this paper is to extract water bodies in very high-resolution aerial image like 20cm or higher resolution. Classification based methods are mostly computationally complex and not suitable for such largely sized data. Contour based methods like level set or Snakes model ask for initial position of contours and also involve the adjustment of many empirical parameters. Under this condition, we propose a novel method with few parameters to automatically detect water bodies with easily computed color feature, disparity feature and matching correlation values.

3. Motivation

High-resolution aerial image provides richer information, but the enormous amount of details makes it more difficult to grasp the semantic knowledge of the objects in the image.

Commonly speaking, in high-resolution aerial image, water bodies appear as dark blue or green region with smooth surface. Sometimes, tides appear as small white pepper noise over the water surface. After all, there is similar and relatively uniform color distribution inside the water region. On the other hand, water bodies appear as noisy regions with uncertain disparity

† NEC System Technologies, Ltd.

values in the disparity image, whatever color the water body is. At the same time, weak texture in water body results in the low matching correlation value between pixels both in water region.

However, other landforms have different characteristics from water bodies. In Table 1, the features of different landforms are listed.

Table 1. Features of different landforms

Landform	Color image	Disparity image	Matching Correlation values
Waters	smooth	noisy	low
Fields	smooth	smooth	low
Forest	textured	smooth	high

4. Automatic Water Body Detection Method

According to the special characteristics of water bodies described above, an automatic method is proposed to detect water bodies in two steps. Firstly, the potential water regions are extracted according to the wavelet based score produced from the color and disparity features. Secondly, only the potential water regions with low matching correlation values are finally decided as the water bodies.

4.1 Disparity feature from stereo images

The accurate disparity image with pixel level precision is not suitable for current application. In such accurate disparity image with great details, though the water bodies appear as noisy regions, there still exist a lot of tiny noise regions because of the original noise in aerial images. In Figure 1(c), we show a disparity image with pixel-level precision, which is generated by the RealScape® stereo processing system [12].

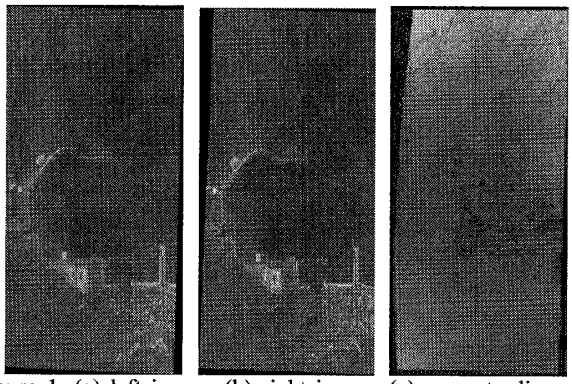

Figure 1, (a) left image, (b) right image, (c) accurate disparity image

To tackle this problem, a disparity estimation method is specifically designed to output a coarse disparity image keeping noisy water regions but without other detailed noise. Note that it is assumed that the left and right images used here have been rectified to assure that corresponding pixels are on the same scanline.

To generate the disparity image suitable for current application, we decide to firstly perform the disparity estimation in shrunk images, and then transfer the above estimated disparity to the original image. After that, the corresponding point searching of each pixel in the original image, that is, the final disparity is calculated under the guidance of the transferred estimation value. In this way, since the initial estimation is carried out in the shrunk image, the disparity noise because of the image details is smoothed out. At the same time, due to the uncertainty of disparity in water bodies, the noise in the water region remains.

Because the disparity estimation is firstly performed in smaller images, it is possible for us to obtain the result efficiently even with a relatively large corresponding point searching range. For example, if the height and width of original images are reduced to the 1/10 of the original ones. The searching range [-100,100] under the shrunk images has the same effect of the range of [-1000, 1000] in the original images. By studying the image pairs, it is easy to set a proper searching range for different stereo image pairs.

To prevent wrong estimations from interfering with the latter processing, it is necessary to pick out occlusion pixels according to the ordering constraints of stereo matching before the disparity propagation. Such occlusion pixels are transferred as the same occlusion pixels in the original images. Then the searching range $[l_i,h_i]$ for non-occlusion pixel i is decided based on the following equations.

$$l_i = D_i - t,\ h_i = D_i + t \quad (1)$$

$$D_i = d_i / r \quad (2)$$

where t decides the searching range around the a priori disparity transferred from the shrunk image. Since the a priori disparity has provided approximately correct initial value, it is proper to set the same value of t for all the pixels. In addition, d_i is the estimated disparity in the shrunk image and r is the size reduction ratio, for example, 1/10.

We show the disparity image generated by the above method in Figure 2(a). As we can see, compared with other terrestrial objects, the water region is full of noise while most of the noise in the mountains disappears. In addition, occlusion pixels are set to a special graylevel 0, shown as black pixels.

4.2 Wavelet based feature analysis

To extract the water regions by the smooth color feature and noisy disparity feature, a score based on the wavelet transform result is proposed and described in this section.

The 2D discrete Haar wavelet transform is applied to an original color image and the coarse disparity image respectively. In the LH, HL, and HH sub-images of color image, the detail responses in water region are not as strong as the other terrestrial objects, such as buildings, trees, roads etc. On the contrary, in those sub-images of coarse disparity image, the responses in water regions are very strong. Based on the above analysis, the following score is proposed.

$$S = \frac{RD_{LH} + RD_{HL} + RD_{HH}}{3} - \frac{RI_{LH} + RI_{HL} + RI_{HH}}{3} \quad (3)$$

In the above equation, S is the detection score on every pixel. Pixels with higher score are much more probable to belong to water bodies. RD_{LH}, RD_{HL}, RD_{HH} respectively represents the response in LH, HL, HH sub-images from disparity image. RI_{LH}, RI_{HL}, RI_{HH} represents those from the color image.

The detection score on every pixel is computed and then normalized to [0,255] to be represented as a score image. For the

image pair of Figure 1(a), (b), and their coarse disparity image Figure 2(a), the detection score image thresholded by an empirical value 128 is shown in Figure 2(b), in which the pixels in water region are shown as white pixels. In this result image, most of the pixels in water regions are detected. However, there are still some water pixels missed, and also some non-water pixels wrongly detected due to the noise in both color and coarse disparity images. To reduce noise, we further extract connected components and remove the small regions. Then among all the connected components, only the segments mainly composed of the water pixels are kept. The remaining segments are called as potential water regions here. The result image after post-processing is shown in Figure 2(c). But there are still some problems in this result. Firstly, since the coarse disparity image is produced based on the initial disparity estimated in a smaller image, the boundary of the regions in the result is not so precise. Secondly, there are still some non-water regions wrongly detected, for example, those in the mountain. To tackle these problems, it is necessary to introduce some new information.

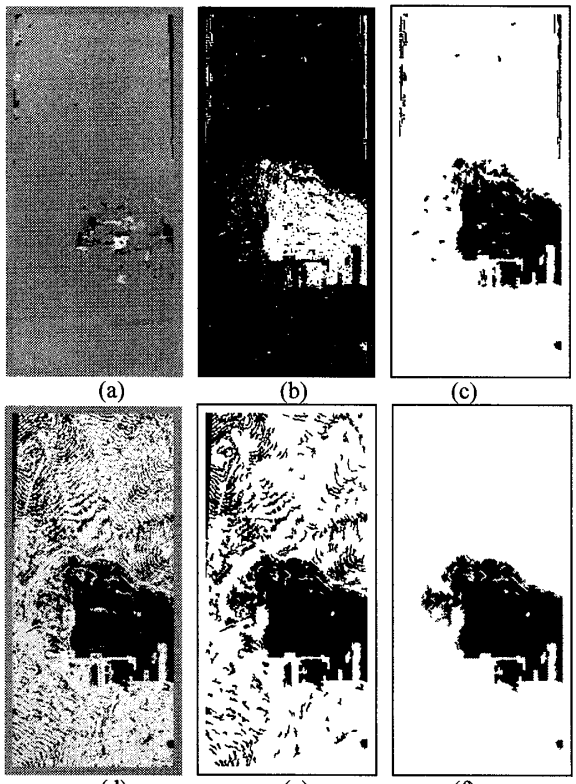

Figure 2, (a) coarse disparity image, (b) thresholded detection score image, (c) potential water regions, (d) normalized disparity image, (e) low matching correlation regions, (f) final result

4.3 Matching correlation value analysis

In order to obtain the more accurate water extraction result, the matching correlation value is introduced to help to make the final decision.

The matching correlation is defined the maximum correlation value between current pixel and another pixel in the given corresponding point searching range. To simplify the processing, we set the same corresponding point searching range for all the pixels in the image. In this case, the range should be set according to the pixels with largest disparity. Otherwise, the matching correlation value for such pixels is also very low because of non-existence of matching point in this range.

We apply the following equation to compute the correlation between the pixels from left and right images.

$$M = \frac{\sum_{i,j}(L_{ij} - \bar{L})(R_{ij} - \bar{R})}{\sqrt{\sum_{i,j}(L_{ij} - \bar{L})^2 \sum_{i,j}(R_{ij} - \bar{R})^2}} \quad (4)$$

The above correlation M is calculated between two windows surrounding the two pixels respectively in left and right images. In this equation, L_{ij} and R_{ij} are the graylevels of pixel (i,j) in left and right images. $\bar{L}$ and $\bar{R}$ are the average graylevel respectively for the windows in two images.

Due to the weak texture in water body, the matching correlation value between the pixels in water body is relatively low compared with those in other landforms. According to our study, the matching correlation values in water region are usually around 0.3~0.5. To assure that the wrongly matched pixels in water region are all extracted, a relatively high threshold 0.8 is applied to all the matching correlation values. By this means, we obtain the image shown in Figure 2(d), in which the pixels with matching correlation value below 0.8 is shown in black region and others are normalized to [1,255] according to the obtained disparity value. To avoid the wrong values caused by the blank regions near the four sides of images, all the following analysis will not be performed in the margin regions along the four sides. As we can see, the margin regions are set as brown regions in the image. From the image, we can find that besides the water region, the occlusion regions in the mountain are also shown as black regions.

This normalized disparity image is then post-processed by the method similar to the thresholded detection score image. That is, connected component extraction, small region elimination and valid segment selection. The remaining segments called as low matching correlation regions are shown in Figure 2(e). For each low matching correlation region, only the segments mainly composed of the potential water region pixels are finally accepted as the water bodies. The final result is shown in Figure 2(f). In this way, the boundary of each extracted water region is much more accurate without interference from the image reduction during coarse disparity image generation.

5. Experimental Analysis

In this section, the experimental results on different images are discussed.

We have shown the result on an example image pair. In this example, the water bodies and the surrounding forest region are similar in color feature. Therefore, it is very difficult to differentiate them from each other simply based on the color information. With the introduction of disparity and matching correlation, the result shows that the proposed method successfully detects the water bodies. Furthermore, a very small water body in the bottom right part is also successfully extracted. This example shows the effectiveness of the proposed method

independent from the color and size varieties of the water bodies. In another example image pair shown in Figure 3(a), (b), the result image Figure 3(f) proves that the proposed method is also effective in detecting water bodies in various shapes.

At the same time, there are still some parts of water bodies are missed with current method. In the first example, there are some small regions in the water body undetected because of the interference of the mud around the marine outfall and the objects used for fish breeding over the water surface. In the second example, the power lines over the river and the stepladders beside the river bank also interfere with the accuracy of the water body detection.

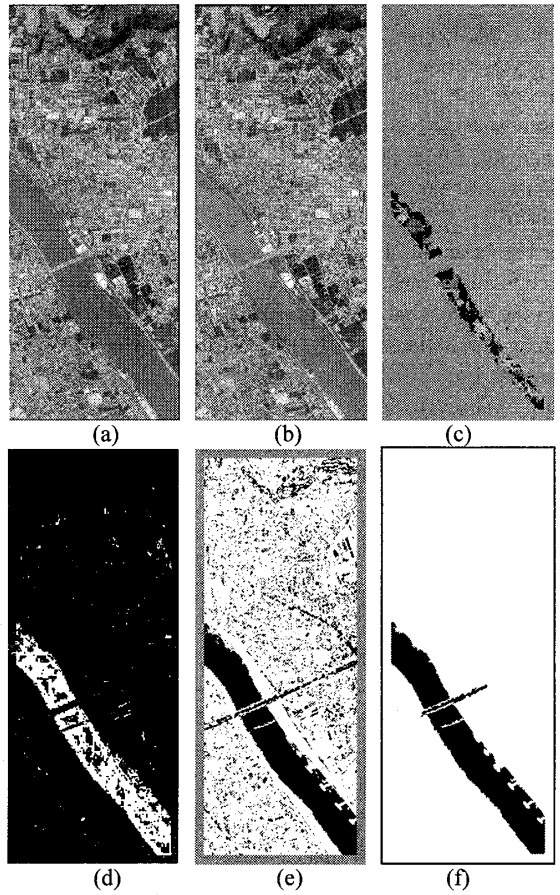

Figure 3, (a) left image, (b) right image, (c) coarse disparity image, (d) thresholded detection score image, (e) normalized disparity image, (f) final result

6 . Conclusion

In this paper, a novel automatic water body detection method is proposed. The experimental results show that the proposed method is able to extract the water bodies with different size, color and shape.

In the future work, the problem of how to include the missed water body parts due to the interference of small objects under or over water surface will be studied. What's more, to assure to obtain the correct result of matching correlation, currently large searching range is used. To improve the efficiency, it is necessary to design the adaptive searching range for each pixel in further research.

Acknowledgement

The authors gratefully acknowledge the provision of the original data in Figure 3 by Wesco Incorporation, Japan.

References

[1] Meichun Yan, Liliang Ren, Xiufeng He, Wengang Sang. Evaluation of Urban Environmental Quality with High Resolution Satellite Images. IEEE International Geoscience and Remote Sensing Symposium 2008(IGARSS 2008), 3:1280-1283, 2008.

[2] Liu Chih-Heng, Chou Tien-Yin, Yang Lung-Shin. The Study of Water Source Preventation and Monition by Using Grid Conception and RS Satellite Image Classification. The 2nd International Conference on Bioinformatics and Biomedical Engineering 2008(ICBBE 2008), 2914-2917, 2008.

[3] Kummu, M., Lu, X.X., Rasphone, A., Sarkkula, J. and Koponen, J. Riverbank changes along the Mekong River: Remote Sensing Detection in the Vientiane-Nong Khai Area. Quaternary International, 186(1): 100-112, 2008.

[4] Vanderbrug, G.J. Line Detection in Satellite Imagery. IEEE Transactions on Geoscience Electronics, 14(1): 37-44, 1976.

[5] Bajcsy, R. and Tavakoli, M. Computer recognition of roads from satellite pictures, Proc. of Second Inter. Joint Conf. on Pattern Recognition, 190-194, 1974.

[6] Pierre Soille, Jacopo Grazzini. Extraction of River Networks from Satellite Images by Combining Mathematical Morphology and Hydrology. Computer Analysis of Images and Patterns. 4673/2007:636-644, 2007.

[7] Qiming QIN ,Yinhuan YUAN, Rongjian LU. A New Approach to Object Recognition on High Resolution Satellite Image. International Archives of Photogrammetry and Remote Sensing(isprs), XXXIII(B3):753-760. 2000.

[8] Geneletti D., Gorte B. G. H. A Method for Object-oriented Land Cover Classification Combining Landsat TM Data and Aerial Photographs. International journal of remote sensing, 24(6):1273-1286, 2003.

[9] Rajiv Kumar Nath, S K Deb. Water-Body Area Extraction from High Resolution Satellite Images-An Introduction, Review, and Comparison. International Journal of Image Processing, 3(6):353-372, 2010.

[10] Zhang Yanling, Liu Zhengjun, Zhang Jixian, Yan Haowen. Water Extraction from High Resolution Satellite Image Based on the Fast Matching Level Set Method. International Conference on Geo-spatial Solutions for Emergency Management, XXXVIII-7/C4: 326-329, 2009.

[11] Craig R. Dillabaugh, K. Olaf Niemann, Dianne E. Richardson. Semi-Automated Extraction of Rivers from Digital Imagery. GeoInformatica, 6(3): 263-284, 2002.

[12] Hirokazu Koizumi, Hiroyuki Yagyu, Kazuaki Hashizume, Toshiyuki Kamiya, Kazuo Kunieda, Hideo Shimazu. Metropolitan Fixed Assets Change Judgment using Aerial Photographs. Proc. of the 21st Innovative Applications of Artificial Intelligence Conference 2009, 17-24, 2009.